Journal of Solid State Chemistry 184 (2011) 1286–1292

Contents lists available at ScienceDirect

Journal of Solid State Chemistry

journal homepage: www.elsevier.com/locate/jssc

Synthesis of carbon nanotube/anatase titania composites by a combination of sol–gel and self-assembly at low temperature

Changyuan Hu [a,b,*], Rongfa Zhang [a,b], Junhuai Xiang [a,b], Tingzhi Liu [a,b], Wenkui Li [a,b], Mingsheng Li [a,b], Shuwang Duo [a,b], Fei Wei [c,d,**]

[a] Jiangxi Key Laboratory of Surface Engineering, Jiangxi Science and Technology Normal University, Nanchang 330013, P.R. China
[b] School of Materials Science and Engineering, Jiangxi Science and Technology Normal University, Nanchang 330013, P.R. China
[c] Beijing Key Laboratory of Green Chemical Reaction Engineering and Technology, Tsinghua University, Beijing 100084, P.R. China
[d] Department of Chemical Engineering, Tsinghua University, Beijing 100084, P.R. China

ARTICLE INFO

Article history:
Received 28 November 2010
Received in revised form
24 March 2011
Accepted 26 March 2011
Available online 6 April 2011

Keywords:
TiO_2
Carbon nanotubes
Sol–gel
Self-assembly
Photodegradation
Methyl orange

ABSTRACT

A simple method is described for the synthesis of carbon nanotube/anatase titania composites by a combination of a sol–gel method with a self-assembly technique at 65 °C. This method makes use of polyelectrolyte for wrapping multi-walled carbon nanotube (MWCNT) and providing them with adsorption sites for electrostatically driven TiO_2 nanoparticle deposition. The composites were characterized using X-ray diffraction, transmission electron microscopy, Fourier transform infrared and X-ray photoelectron spectroscopy, and photoluminescence for analyzing their crystal phase, microstructure, particle size, and other physicochemical properties. The results showed that MWCNT were covered with an anatase TiO_2 thin layer or surrounded by an anatase TiO_2 thick coating, which is constructed of TiO_2 particles about 6 nm in size. The composites were rich in surface hydroxyl groups. The excited e^- in conduction band of TiO_2 may migrate to MWCNT. Concerning the potential applicability, MWCNT/TiO_2 composites showed excellent photocatalytic activity toward the photodegradation of methyl orange.

1. Introduction

Increasing interest has been drawn in carbon nanotube (CNT) due to their unique structural, the resultant electrical, mechanical properties, and wide scope of possible applications [1]. CNT coated with metal oxides are expected to exhibit different physical, chemical, and mechanical properties than those of neat CNT, and they may be proven to be key components in fields such as energy conversion [2], sensors [3,4], hydrogen storage [5], and catalysts [6]. Among the metal oxides investigated, TiO_2 has recently been the focus of much research due to its photocatalytic activity. However, the photocatalytic activity of pure TiO_2 is not high enough for practical applications [7]. Among the possible materials proposed for modifying TiO_2, CNT are highly promising due to their unique structure and properties [6,8,9].

Up to now, considerable efforts have been dedicated to combine TiO_2 with CNT in simple mixtures or as composites materials for creation more highly reactive photocatalysts [8–10]. The synthesis of CNT/TiO_2 composites using sol–gel, vapor phase method, self-assembly, and so on has been reported [11–19]. For instance, a TiO_2 thin layer or TiO_2 nanoparticle coated multi-walled carbon nanotube (MWCNT) composites was obtained by the sol–gel method [16,17]. The controlled synthesis of anatase TiO_2 coated MWCNT was carried out by vapor phase method [14]. Anatase TiO_2 nanoparticles were covalently anchored onto acid-treated MWCNT through a nanocoating-hydrothermal process to obtain MWCNT/TiO_2 composites [18]. Li et al. [15] devised a self-assembly approach for preparation of CNT/TiO_2 composites using pre-synthesized TiO_2 nanoparticles as primary building units. Liu and Zeng [19] have developed a one-pot chemical approach to prepare mesocrystals of anatase TiO_2 on MWCNT. However, the above mentioned synthesis of CNT/TiO_2 composites involved expensive TiF_4 reagents, toxic HF gas release [19], pre-synthesis and treatment of TiO_2 with expensive and toxic reagents, such as toluene and oleic acid [15], high temperature thermal treatment for transforming the amorphous oxide into anatase TiO_2 [12,17]. Overall, it is still a challenge to synthesize CNT/TiO_2 hybrids via *in situ* deposition of nanocrystals onto CNT under mild conditions.

* Corresponding author at: Jiangxi Key Laboratory of Surface Engineering, Jiangxi Science and Technology Normal University, Nanchang 330013, P.R. China. Fax: +86 791 3831266.
** Corresponding author at: Beijing Key Laboratory of Green Chemical Reaction Engineering and Technology, Department of Chemical Engineering, Tsinghua University, Beijing 100084, P.R. China. Fax: +86 1062772051.
E-mail addresses: hcy6257@163.com (C. Hu), wf-dce@tsinghua.edu.cn (F. Wei).

0022-4596/$ - see front matter © 2011 Elsevier Inc. All rights reserved.
doi:10.1016/j.jssc.2011.03.040

Therefore, it is necessary to find an efficient and easy way to synthesize and attach anatase TiO_2 onto CNT in one step under mild conditions. One of the techniques offering very broad applicability is the layer-by-layer (LBL) assembly, which is mainly based on the use of polyelectrolyte as molecular glue between the substrate and nanoparticle or between successive nanoparticle layers [20]. The assembly of semiconductor particles onto CNT is an attractive method for forming such heterogeneous structures [3]. Recently, we have synthesized nanocrystalline anatase TiO_2 without high temperature calcination, by an effective sol–gel method through the control of pH at 65 °C [21]. In this paper, MWCNT/anatase TiO_2 composites were investigated by the combination of above sol–gel method and LBL technique in one step at 65 °C. To successfully attach TiO_2 onto MWCNT, two kinds of polyelectrolyte, poly(diallyldimethylammonium chloride) (PDDA) and poly(sodium 4-styrenesulfonate) (PSS), were first sequentially LBL assembled onto MWCNT, thus enabling MWCNT to be negatively charged. Compared to widely adopted sol–gel [12,17] or self-assembly [15] method, the primary differences and advantages of this effective method are shown below. First, nanocrystalline anatase TiO_2 can be synthesized at 65 °C by an easy sol–gel method through the control of pH 1.5 without high temperature calcination. Furthermore, thus synthesized TiO_2 are positively charged, because the pH 1.5 is lower than the isoelectric point of TiO_2 (pH 5–7). Second, this method makes use of polyelectrolyte for not only wrapping MWCNT to disperse them well, but also providing them with adsorption sites for electrostatically driven nanoparticle deposition, which ensures that the positively charged titania sol formed *in situ* can be rapidly captured by negatively charged MWCNT through electrostatic interaction, whilst the homogeneous nucleation of titania can be minimized. Third, the formation and assembly of anatase TiO_2 onto MWCNT can be completed in one-pot, without pre-synthesis of TiO_2 particles and special equipment under environmental benign conditions. Fourth, thus synthesized MWCNT/TiO_2 composites are rich in surface hydroxyl groups, which play an important role in the photocatalytic degradation.

2. Experimental section

2.1. Materials

PDDA and PSS are purchased from Sigma-Aldrich. Other reagents used are A.R. grade and purchased from Shanghai Chemical Company of China. MWCNT with a purity of about 95% are provided by Shenzhen Nanoport Company (Senzhen, China).

2.2. Preparation of samples

Initially, MWCNT was refluxed in concentrated nitric acid for 10 h to purify received samples. PDDA, 20 wt% in water, Mw=400,000–500,000, and PSS, Mw=70,000, are used as received. PDDA and PSS were dissolved in de-ionized water at a concentration of 5 mg/mL, containing 0.1 M NaCl, for LBL assembly. Four layers of PDDA/PSS/PDDA/PSS, were first sequentially coated onto MWCNT by LBL assembly, which forms the outermost layer of PSS, thus enabling MWCNT to be negatively charged [22].

To synthesize MWCNT/TiO_2 composites, a typical procedure is as follows: tetrabutyl titanate ($Ti(OBu)_4$) (6.4 mL) and glacial acetic acid (3.2 mL) were mixed under stirring at room temperature (RT) for 30 min to restrain the intensive hydrolysis of $Ti(OBu)_4$. After that, anhydrous ethanol (10.89 mL) was added to the $Ti(OBu)_4$/glacial acetic acid mixture and stirred at RT for another 10 min. The obtained mixture solution was named as S_A. Expected amount of polyelectrolyte pretreated MWCNT were sonicated in the mixture of anhydrous ethanol (54.45 mL) and de-ionized water (2.03 mL) for 20 min to disperse them well. By adding 4 M HNO_3 to the suspension of MWCNT until the final pH 1.5 was obtained under stirring at RT, the obtained suspension of MWCNT was named as S_B. S_A was added drop by drop to S_B under vigorous stirring at RT. The final pH was adjusted again to 1.5 by adding 4 M HNO_3 to the mixed solution of S_A and S_B. The solution was kept under strong stirring at RT for 4 h, and then heated by water bath at 65 °C for 20 h under stirring to form MWCNT/TiO_2 composites *in situ*. The products were separated by centrifugation and then washed with de-ionized water. Finally, the samples were dried in an oven at 120 °C for 24 h. The obtained products were named as *x*%MWCNT/TiO_2. Herein, *x*% is the weight ratio of MWCNT/TiO_2 (x=10, 20, 30).

2.3. Characterization of samples

The X-ray powder diffraction (XRD) patterns were obtained on a Rigaku X-ray diffractometer to determine the crystallite size and identity of TiO_2 samples. The microscopic structures, energy dispersive X-ray (EDX) spectrum and selected area electron diffraction (SAED) of composites were investigated with a JEM 2100 transmission electron microscope (TEM). The surface functional groups of samples were examined by the KBr pellet method on a Brueker vertex 70 Fourier transform infrared (FTIR) spectrometer in the wavenumber range 4000–400 cm^{-1}. The X-ray photoelectron spectroscopy (XPS) measurement was made on a KRATOS Analytical AXISHSi spectrometer with a monochromatized Al $K\alpha$ X-ray source (1486.6 eV photons). The binding energy scale was calibrated by the Au 4*f* 7/2 peak at 83.9 eV as well as Cu 2*p* 3/2 peak at 76.5 and 932.5 eV. Room temperature photoluminescence (PL) spectroscopy measurement at 325 nm excitations was performed using F-4600.

2.4. Photocatalytic activity measurement

Photocatalytic performance of MWCNT/TiO_2 composites was studied by degradation of methyl orange (MO) as a target pollutant. In a typical process, 20 mg 10% MWCNT/TiO_2 was added to 100 mL 15 mg/L MO solution with a catalyst concentration of 0.2 mg/mL, and then magnetically stirred in the dark for 1 h, which allows composites to reach an adsorption equilibrium; then the above mixture was exposed to UV irradiation by a 250-W high-pressure Hg lamp at room temperature. Aeration was performed by an air pump to ensure a constant supply of oxygen and promoted complete mixing of solution and photocatalysts during photoreaction. The sample was collected by centrifugation at given time intervals to measure MO concentration by UV–vis spectroscopy at 464.2 nm.

3. Results and discussion

3.1. XRD patterns

Fig. 1 shows the XRD patterns of acid-treated MWCNT and MWCNT/TiO_2 composites. The MWCNT present intense peak assigned to the (0 0 2) reflection (Fig. 1d). In the case of the composites (Fig. 1a–c), it is hard to elicit the characteristic peak of MWCNT from the spectrum of composites because of the good crystallization of anatase TiO_2 (JCPDS card no. 78-2486) and their fine attachment onto MWCNT. The width of the reflections is considerably broadened, indicating a small crystalline domain size, which can be roughly quantified by Scherrer's equation. According to Debye–Scherrer formula, the average crystallite size

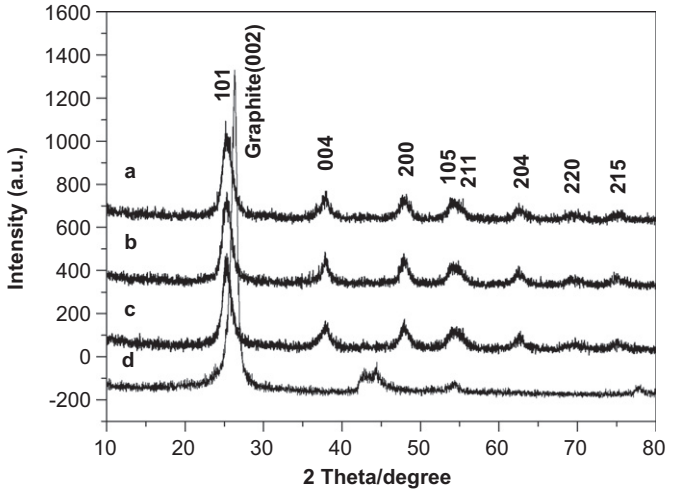

Fig. 1. XRD patterns of samples (a: 10%MWCNT/TiO_2, b: 20% MWCNT/TiO_2, c: 30% MWCNT/TiO_2, d: acid-treated MWCNT).

of TiO_2 on the surface of MWCNT for 10% MWCNT/TiO_2, 20% MWCNT/TiO_2, and 30% MWCNT/TiO_2 is 6.2, 5.7, and 5.9 nm, respectively.

3.2. TEM analysis

The direct evidence of the formation of TiO_2 nanoparticles on the surface of MWCNT is given by TEM images. Fig. 2 shows the morphological, structural characterizations of MWCNT/TiO_2 composites. The images reveal that most of the MWCNT have been covered with a TiO_2 thin layer (marked 1) or surrounded by a TiO_2 thick coating (marked 2). It should be noted that the layer/coating is constructed of TiO_2 particles about 6 nm (determined by TEM in Fig. 2b, d, f) in diameter, which is consistent with the XRD results. Energy dispersive X-ray (EDX) spectrum analysis of MWCNT/TiO_2 samples (Fig. 3a–c) clearly reveals the presence of C, O, and Ti elements, also indicating the actual deposition of TiO_2 on MWCNT. The structure of the TiO_2 powders is further confirmed to be the anatase phase by selective area electron diffraction (SAED) as

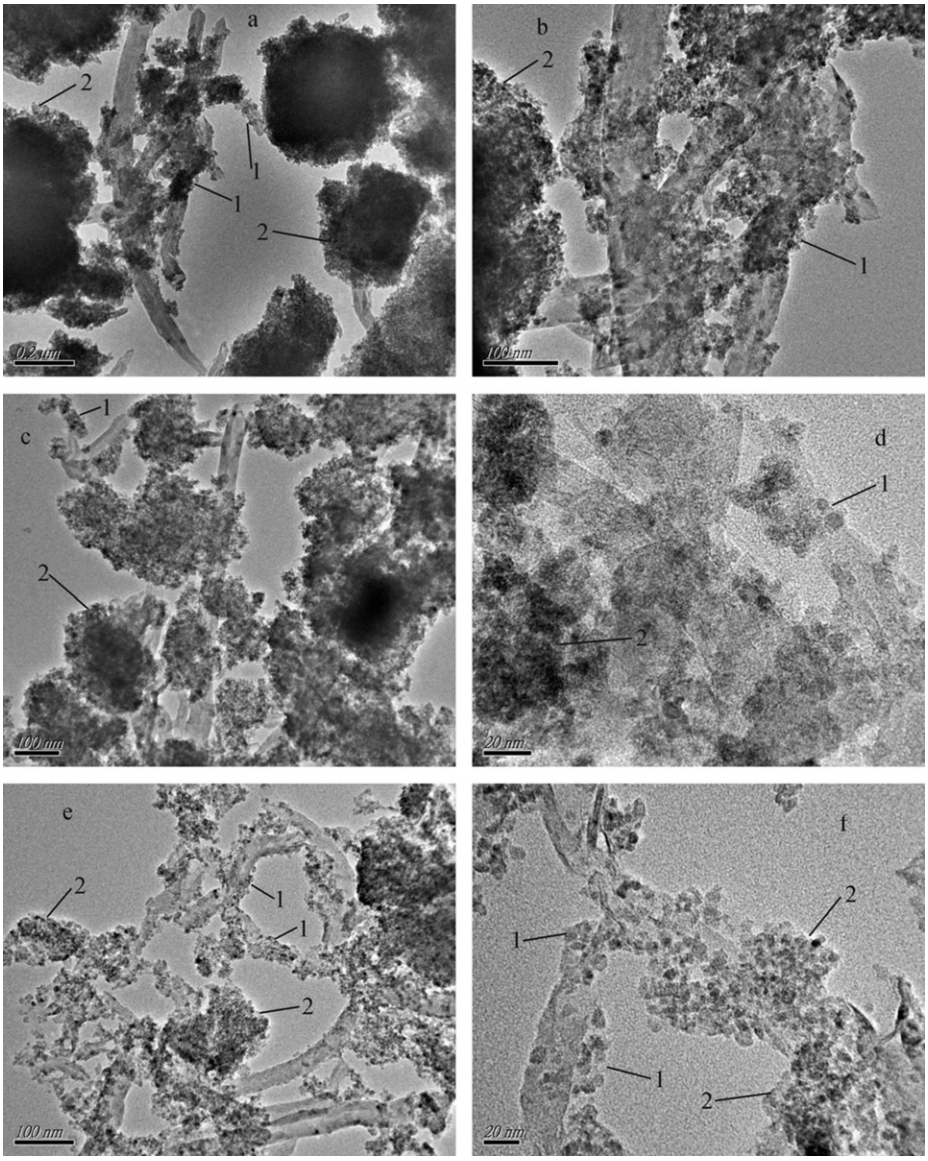

Fig. 2. TEM images of (a, b) 10%MWCNT/TiO_2; (c, d) 20% MWCNT/TiO_2; (e, f) 30% MWCNT/TiO_2, respectively. Figures on the right have higher resolutions.

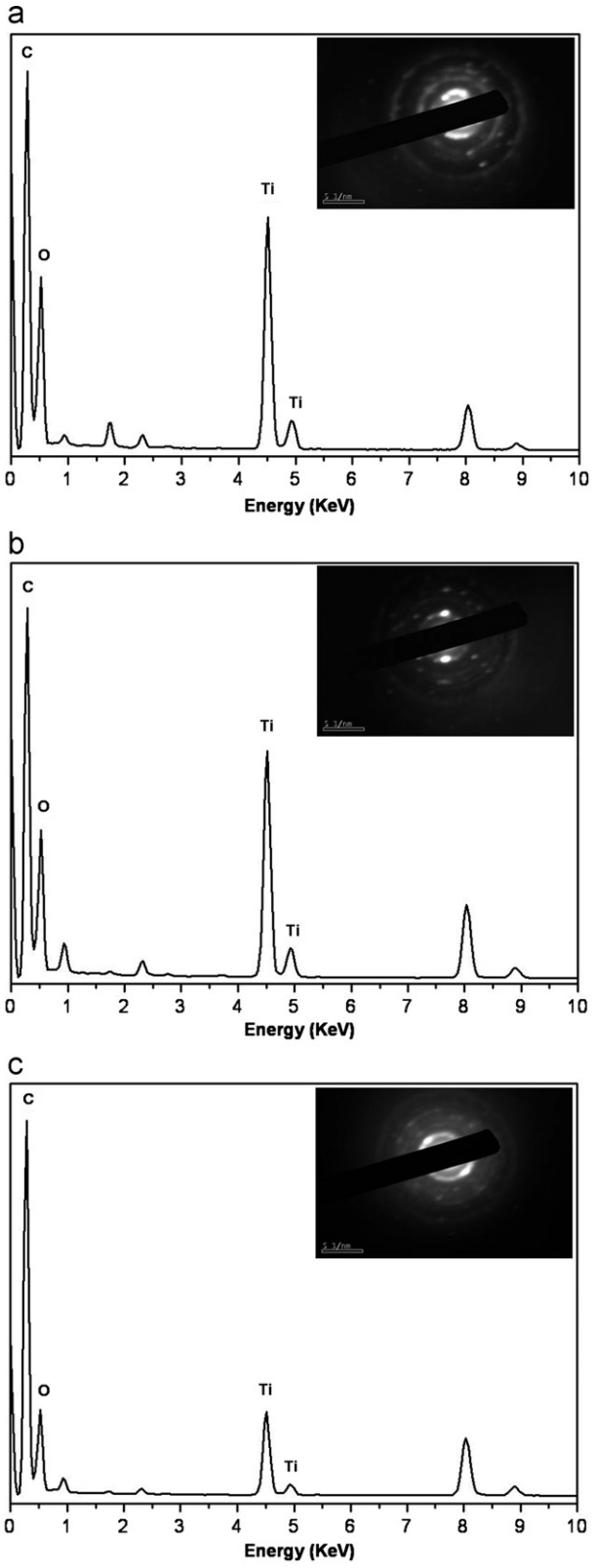

Fig. 3. EDX spectrum and SAED patterns of samples (a: 10% MWCNT/TiO_2, b: 20% MWCNT/TiO_2, c: 30% MWCNT/TiO_2).

shown in the inset [19], located on the top right corner of Fig. 3a–c, in agreement with the X-ray diffraction data. pH control to a relatively low value is crucial to facilitate the formation of crystalline TiO_2 on MWCNT. The growing crystalline TiO_2 species such as $[Ti(OH)_x(OH_2)_{6-x}]^{(4-x)+}$ are positively charged [23], as pH 1.5 in our experiment is lower than the isoelectric point of TiO_2 (pH 5–7) [24]. Thus, the negatively charged surface of MWCNT pretreated by four layers of PDDA/PSS/PDDA/PSS polyelectrolyte, adsorb rapidly the positively charged growing crystalline TiO_2 species due to electrostatic attraction, which induces the TiO_2 nanocrystals to grow onto MWCNT *in situ*. Continuous adsorption of titania particles on the initially formed TiO_2 resulted in remarkably large thickness of the TiO_2 layer. The aggregation of TiO_2 nanoparticles indicates the supporting role of MWCNT as centers for the deposition and growth of hydrolysis products, as well as, the support for spatial confinement of the TiO_2 clusters [6]. However, the distribution of the TiO_2 clusters is far from being homogenous. Further efforts are needed to optimize experimental parameters for the synthesis of smooth, homogeneous titania coatings on the surface of MWCNT.

3.3. FTIR spectra

FTIR spectra provide information of surface functional groups. The spectra are an effective method to study adsorbed species on solid surfaces. As shown in Fig. 4d, MWCNT exhibited characteristic absorption bands for PSS and PDDA. The relatively weak bands at 2925 and 2846 cm^{-1} are attributed to the stretching vibrations of the CH_3– and –CH_2– groups, respectively [25,26]. The peaks in the range of 1645–1400 cm^{-1} are attributed to the bending modes of aromatic rings [26,27]. The bands in the range of 1200–1000 cm^{-1} are assigned to vibration of S=O groups [26,27]. These results indicate that the PSS and PDDA were adsorbed onto the surface of MWCNT via LBL assembly. Additionally, the spectra of MWCNT clearly show the presence of OH groups centered at 3406 cm^{-1} resulting from the HNO_3 oxidation. For MWCNT/TiO_2 composites, as shown in Fig. 4a–c, a broad band peak centered at 3406 cm^{-1} is attributed to the OH stretching of physisorbed water on the composites surface, and a relatively sharp band at 1630 cm^{-1} corresponds to the OH bending modes of water molecules [28]. Furthermore, the intensity of OH peaks for MWCNT/TiO_2 composites was far higher than that of MWCNT. From these, the FTIR spectra strongly indicated the presence of abundant hydroxyl groups on composites surface prepared at low temperature, which plays an important role in the photocatalytic degradation. Quantitative analysis of hydroxyl groups will be further addressed in the XPS spectra below. The peak at 1382 cm^{-1} could be assigned to the stretching vibrations of –CH_3 groups [29]. The strong absorption observed below

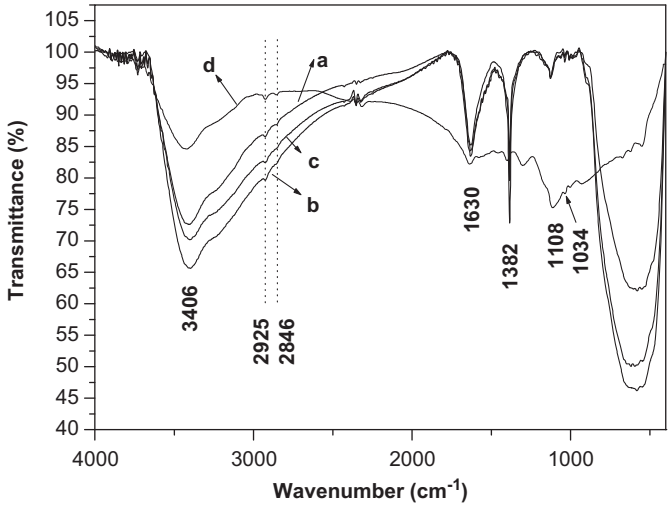

Fig. 4. FTIR spectra of samples (a: 10%MWCNT/TiO_2, b: 20% MWCNT/TiO_2, c: 30% MWCNT/TiO_2, d: polyelectrolyte-treated MWCNT).

850 cm^{-1} could be attributed to the absorption of Ti–O–Ti, which indicates the formation of titania [30].

3.4. XPS spectra

The results of FTIR are supported by the XPS spectroscopy presented in Fig. 5. XPS measurements were carried out to study the Ti, O, C chemical state of the MWCNT/TiO_2 composites. Fig. 5 shows the XPS data for Ti, O, and C core levels of three MWCNT/TiO_2 samples. The formation of the TiO_2 on the sidewall surface of MWCNT is shown clearly by the high-resolution XPS spectra of Ti 2*p* (Fig. 5(1)), which shows the core level spectral values. As shown in Fig. 5(1), the binding energies of Ti $2p_{3/2}$ and $2p_{1/2}$ were centered at 459.1–459.2 and 464.6–464.9 eV for MWCNT/TiO_2, respectively. This clearly revealed that the titanium elements were in the oxidation state IV, corresponding to Ti^{4+}(TiO_2) [31]. Compared with the Ti 2*p* binding energies of TiO_2 (Ti $2p_{3/2}$: 458.6 eV, Ti $2p_{1/2}$: 464.2 eV) obtained by analogous method [21], there are 0.5–0.6 eV positive shifts of Ti $2p_{3/2}$ and 0.4–0.7 eV positive shifts of Ti $2p_{1/2}$ for MWCNT/TiO_2 composites. It was found that the O 1*s* spectra could be fitted to three peaks. The main peak at 530.3–530.6 eV was assigned to lattice oxygen in anatase TiO_2. The other two peaks with higher binding energies located at 531.6–531.7 and 532.9–533.2 eV were attributed to O–H and the C═O groups, respectively [31,32]. Similar to their Ti 2*p* spectra, O 1*s* peaks from the MWCNT/TiO_2 composites are also shifted toward higher binding energies. For example, the lattice oxygen in anatase TiO_2 of composites is now about 0.45–0.75 eV

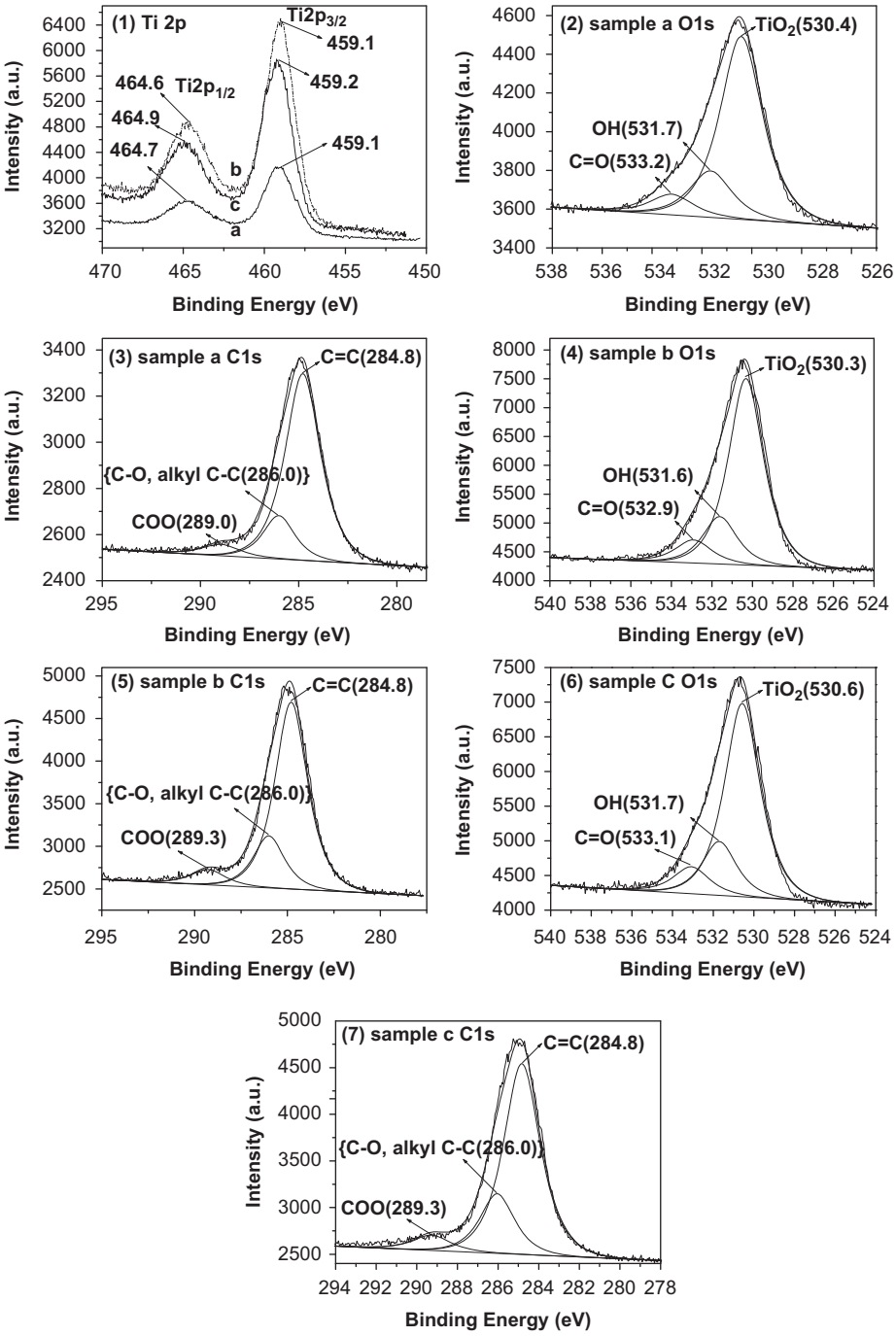

Fig. 5. High-resolution XPS spectra of Ti 2*p*, O 1*s*, and C 1*s* (a: 10% MWCNT/TiO_2, b: 20% MWCNT/TiO_2, c: 30% MWCNT/TiO_2).

higher than that in the pure TiO_2 [21]. The observed binding energies shifts in Ti 2*p* and O 1*s* spectra are primarily due to electronic interaction between the surface TiO_2 and MWCNT substrate (i.e., charge transfer from the surface TiO_2 to MWCNT) [15,33]. The contribution of O–H in three oxygen species, expressed by XPS areas ratio, was as high as 18.53%, 18.14%, and 19.08% for 10% MWCNT/TiO_2, 20% MWCNT/TiO_2, and 30% MWCNT/TiO_2, respectively. Hydroxyl groups existing in the samples are attributed to the chemisorbed H_2O. Although some H_2O is easily adsorbed on the surface of the samples, the physically adsorbed water on the samples is desorbed under the ultra-high vacuum condition of the XPS system. Therefore, XPS spectra only show chemisorbed H_2O [8]. Similarly, the C 1*s* peaks could be fitted to three peaks. The main broad peak of samples centered at 284.8 eV originated from extensively delocalized sp^2-hybryidized graphitelike carbon atoms, assigned as C=C from CNT. The peak at 286.0 eV corresponded to alkyl C–C groups of the adsorbed polyelectrolyte and also C atoms in etherlike (C–O) linkages. The carbon atoms in carboxylic acid groups show small shoulder peaks located at 289.0–289.3 eV [15,34,35]. These results provide further evidence that polyelectrolyte was absorbed onto MWCNT through LBL assembly, and TiO_2 was formed on the surface of MWCNT, and as-prepared MWCNT/TiO_2 composites were rich in surface hydroxyl groups, which supports the results of FTIR. The abundant hydroxyl groups on the surface of composites could promote photocatalytic activity [36,37].

3.5. PL emission spectra

PL spectroscopy is a powerful tool for understanding the electro-optic and photoelectric properties of materials and for investigating the fate of electron-hole pairs in semiconductor particles because PL emission resulted from the recombination of free carriers [38]. Fig. 6 shows the PL spectra of 10% MWCNT/TiO_2 with excitation wavelengths of 325 nm. It was reported that MWCNT gave no PL signal in the measured region [10,39]. The MWCNT/TiO_2 composites feature a broad emission including three observed peaks from 350 to 550 nm, which is attributed to the emission signal of TiO_2 particles. The main peak at 367 nm is likely to have originated from the self-trapped excitons localized on TiO_6 octahedral [38,40]. The 526 nm band should originate from the F^+-type (an oxygen-ion vacancy occupied by one electron centers) color center on the surface of TiO_2 while the 467 nm band should originate from another kind of oxygen vacancy (*F*) (an oxygen-ion vacancy occupied by two electron) [41]. The PL spectra response is relatively broad, indicating that there is a significant ground state interaction between TiO_2 nanoparticles and MWCNT [42]. It can be concluded that electrons from the external TiO_2 nanoparticles will flow into the inner MWCNT, forming an accumulation layer of electrons.

3.6. Photocatalytic performance

To test the potential application of the above prepared MWCNT/TiO_2 composites in real working environments, we selected the 10% MWCNT/TiO_2 as an example for MO photodegradation. Fig. 7 shows the evolution curves of MO photodegradation on 10% MWCNT/TiO_2. As shown in Fig. 7, the concentration of MO decreases heavily as the exposure time increases. After exposure for 30 min, 96.4% MO was photo-degraded and MO completely disappeared after 40 min exposure. To obtain a quantitative understanding on the reaction kinetics of the MO degradation, we apply the pseudo-first order model as expressed by equation $\ln(C_0/C)=kt$, which is generally used for photodegradation if the initial concentration of pollutant is low [43]: where C_0 and C are the concentrations of dye in solution at time 0 and t, respectively, and k is the pseudo-first-order rate constant. The inset in Fig. 7 depicts the photocatalytic reaction kinetics of MO degradation in solution. A rather good correlation to the pseudo-first-order reaction kinetics ($R>0.98$) was found from these results. The reaction constant k is 0.1299 min^{-1}, indicating that the 10% MWCNT/TiO_2 composites have great photocatalytic activity toward the photodegradation of MO. As mentioned above, MWCNT–TiO_2 composites are rich in surface hydroxyl groups. Furthermore, electronic interaction between the surface TiO_2 and MWCNT substrate could occur for composites. The abundant hydroxyl groups adsorbed on the surface of composites can lead to the formation of considerable hydroxyl radicals, which oxidizes the adsorbed MO on the surface [44]. Due to the electronic interaction between TiO_2 and MWCNT, the excited e^- in conduction band of TiO_2 may migrate to MWCNT with transporting e^- ability, so that the possibility of recombination of the e^-/h^+ pairs decreases [8,10]. Moreover, the MWCNT/TiO_2 composites have the higher surface area-to-volume ratios allowing for greater photon absorption on the photocatalyst surface [3,45]. Therefore,

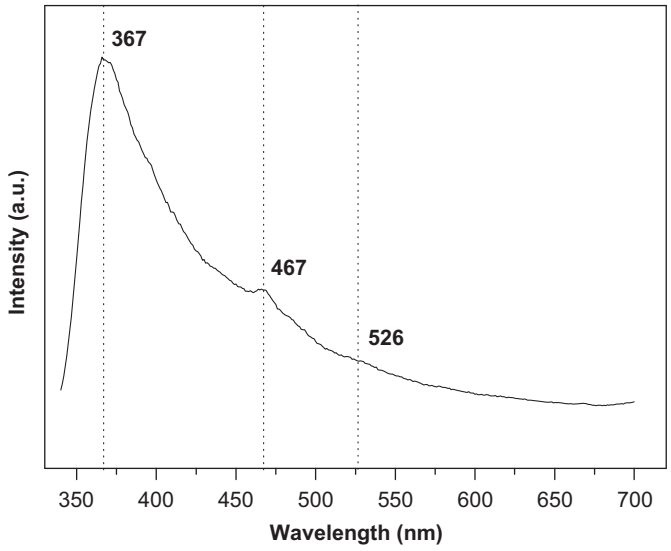

Fig. 6. PL spectra of 10% MWCNT/TiO_2.

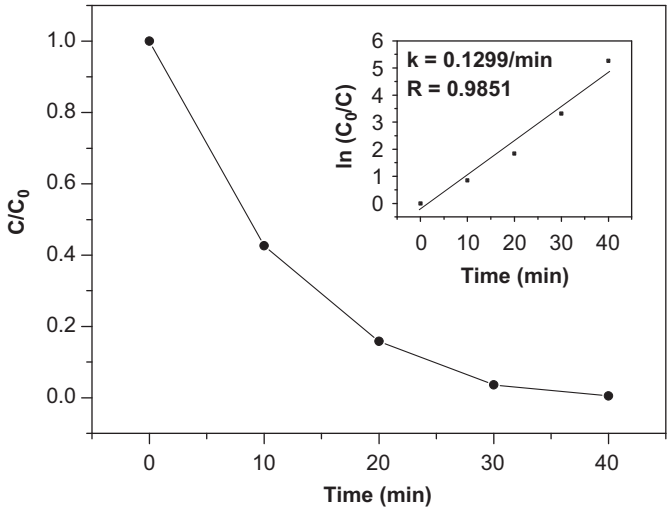

Fig. 7. MO photodegradation over 10% MWCNT/TiO_2 under UV-light irradiation, and photocatalytic reaction kinetics of MO decomposition (inset).

MWCNT/TiO_2 composites show great photocatalytic activity through the above three aspects.

4. Conclusions

MWCNT/TiO_2 composites have been prepared by a combination of a sol–gel method through the control of pH with a layer-by-layer assembly technique in one step at 65 °C. MWCNT were covered with an anatase TiO_2 thin layer or surrounded by an anatase TiO_2 thick coating, which is constructed of TiO_2 particles about 6 nm in size. The composites were rich in surface hydroxyl groups. The photoluminescence bands showed spectral lines at about 367, 467, and 526 nm, which are attributed to the self-trapped excitons, F and F^+ centers. The excited e^- in conduction band of TiO_2 may migrate to MWCNT. Concerning the potential applicability, MWCNT/TiO_2 composites showed excellent photocatalytic activity toward the photodegradation of methyl orange.

Acknowledgments

This work was partially supported by the National Natural Science Foundation of China (50963003). This work was also financially supported by the Natural Science Foundation of Jiangxi Province (No 2008GQH0021), and the Scientific and Technological Project of Education Department of Jiangxi Province (No GJJ10598).

References

[1] X.S. Qi, Y. Yang, W. Zhong, Y. Deng, C.T. Au, Y.W. Du, J. Solid State Chem. 182 (2009) 2691–2697.
[2] Z. Chen, Y.C. Qin, D. Weng, Q.F. Xiao, Y.T. Peng, X.L. Wang, H.X. Li, F. Wei, Y.F. Lu, Adv. Funct. Mater. 19 (2009) 3420–3426.
[3] M. Sánchez, M.E. Rincón, Sens. Actuators B 140 (2009) 17–23.
[4] S. Santangelo, G. Messina, G. Faggio, A. Donato, L. De Luca, N. Donato, A. Bonavita, G. Neri, J. Solid State Chem. 183 (2010) 2451–2455.
[5] H.S. Kim, H. Lee, K.S. Han, J.H. Kim, M.S. Song, M.S. Park, J.Y. Lee, J.K. Kang, J. Phys. Chem. B 109 (2005) 8983–8986.
[6] B. Gao, G.Z. Chen, G.L. Puma, Appl. Catal. B 89 (2009) 503–509.
[7] C. Minero, D. Vione, Appl. Catal. B 67 (2006) 257–269.
[8] Y. Yu, J.C. Yu, J.G. Yu, Y.C. Kwok, Y.K. Che, J.C. Zhao, L. Ding, W.K. Ge, P.K. Wong, Appl. Catal. A 289 (2005) 186–196.
[9] G.D. Jiang, Z.F. Lin, L.H. Zhu, Y.B. Ding, H.Q. Tang, Carbon 48 (2010) 3369–3375.
[10] Y. Yu, J.C. Yu, C.Y. Chan, Y.K. Che, J.C. Zhao, L. Ding, W.K. Ge, P.K. Wong, Appl. Catal. B 61 (2005) 1–11.
[11] C.Y. Hu, S.W. Duo, T.Z. Liu, W.K. Li, R.F. Zhang, Mater. Lett. 64 (2010) 2472–2474.
[12] S.H.S. Zein, A.R. Boccaccini, Ind. Eng. Chem. Res. 47 (2008) 6598–6606.
[13] D.J. Cooke, D. Eder, J.A. Elliott, J. Phys. Chem. C 114 (2010) 2462–2470.
[14] W.G. Fan, L. Gao, J. Sun, J. Am. Ceram. Soc. 89 (2006) 731–733.
[15] J. Li, S.B. Tang, L. Lu, H.C. Zeng, J. Am. Chem. Soc. 129 (2007) 9401–9409.
[16] P. Vincent, A. Brioude, C. Journet, S. Rabaste, S.T. Purcell, J. Le Brusq, J.C. Plenet, J. Non-Cryst. Solids 311 (2002) 130–137.
[17] A. Jitianu, T. Cacciaguerra, M.H. Berger, R. Benoit, F. Béguin, S. Bonnamy, J. Non-Cryst. Solids 345-346 (2004) 596–600.
[18] Q. Wang, D. Yang, D.M. Chen, Y.B. Wang, Z.Y. Jiang, J. Nanopart. Res. 9 (2007) 1087–1096.
[19] B. Liu, H.C. Zeng, Chem. Mater. 20 (2008) 2711–2718.
[20] G. Decher, Science 277 (1997) 1232–1237.
[21] C.Y. Hu, S.W. Duo, R.F. Zhang, M.S. Li, J.H. Xiang, W.K. Li, Mater. Lett. 64 (2010) 2040–2042.
[22] M.A. Correa-Duarte, A. Kosiorek, W. Kandulski, M. Giersig, L.M. Liz-Marzán, Chem. Mater. 17 (2005) 3268–3272.
[23] M. Gopal, W.J. Moberly Chan, L.C. De Jonghe, J. Mater. Sci. 32 (1997) 6001–6008.
[24] E.A. Barringer, H.K. Bowen, Langmuir 1 (1985) 420–428.
[25] J. Chattopadhyay, F. De Jesus Corte, S. Chakraborty, N.K.H. Slater, W.E. Billups, Chem. Mater. 18 (2006) 5864–5868.
[26] K. Katagiri, A. Matsuda, F. Caruso, Macromolecules 39 (2006) 8067–8074.
[27] L. Chen, G.X. Lu, J. Electroanal. Chem. 597 (2006) 51–59.
[28] H. Jensena, A. Solovieva, Z.S. Li, E.G. Søgaard, Appl. Surf. Sci. 246 (2005) 239–249.
[29] D.V. Kozlov, A.V. Vorontsov, P.G. Smirniotis, E.N. Savinov, Appl. Catal. B 42 (2003) 77–87.
[30] Y.J. Jiang, D. Yang, L. Zhang, L. Li, Q.Y. Sun, Y.F. Zhang, J. Li, Z.Y. Jiang, Dalton Trans. (2008) 4165–4171.
[31] Y.J. Jiang, D. Yang, L. Zhang, Q.Y. Sun, X.H. Sun, J. Li, Z.Y. Jiang, Adv. Funct. Mater. 19 (2009) 150–156.
[32] A.M. Venezia, F.L. Liotta, G. Pantaleo, A. Beck, A. Horvath, O. Geszti, A. Kocsonya, L. Guczi, Appl. Catal. A 310 (2006) 114–121.
[33] K.Y. Lee, M. Kim, J. Hahn, J.S. Suh, I. Lee, K. Kim, S.W. Han, Langmuir 22 (2006) 1817–1821.
[34] Q. Wang, Y.C. Han, Y.L. Wang, Y.J. Qin, Z.X. Guo, J. Phys. Chem. B 112 (2008) 7227–7233.
[35] X.B. Yan, B.K. Tay, Y. Yang, J. Phys. Chem. B 110 (2006) 25844–25849.
[36] A. Fujishima, T.N. Rao, D.A. Tryk, J. Photochem. Photobiol. C. Photochem. Rev. 1 (2000) 1–21.
[37] H. Kominami, H. Kumamoto, Y. Kera, B. Ohtani, Appl. Catal. B 30 (2001) 329–335.
[38] L.Q. Jing, Y.C. Qu, B.Q. Wang, S.D. Li, B.J. Jiang, L.B. Yang, W. Fu, H.G. Fu, J.Z. Sun, Sol. Energy Mater. Sol. Cells 90 (2006) 1773–1787.
[39] H.Q. Wu, Q.Y. Wang, Y.Z. Yao, C. Qian, X.J. Zhang, X.W. Wei, J. Phys. Chem. C 112 (2008) 16779–16783.
[40] J.G. Yu, H.G. Yu, B. Chen, X.J. Zhao, J.C. Yu, W.K. Ho, J. Phys. Chem. B 107 (2003) 13871–13879.
[41] X.F. Song, L. Gao, Langmuir 23 (2007) 11850–11856.
[42] S. Bhattacharyya, E. Kymakis, G.A.J. Amaratunga, Chem. Mater. 16 (2004) 4819–4823.
[43] J.M. Herrmann, Y. Ait-Ichou, G. Lassaletta, A. Fernandez, Appl. Catal. B 13 (1997) 219–228.
[44] J.G. Yu, X.J. Zhao, Q.N. Zhao, Thin Solid Films 379 (2000) 7–14.
[45] M.R. Hoffmann, S.T. Martin, W. Choi, D.W. Bahnemannm, Chem. Rev. 95 (1995) 69–96.